Second Life Battery Energy Storage System for Enhancing Renewable Energy Grid Integration

C. Koch-Ciobotaru[1], A. Saez-de-Ibarra[2], E. Martinez-Laserna[2], D.-I. Stroe[3], M. Swierczynski[3], P. Rodriguez[1]

[1]Abengoa Research
Seville, Spain
Cosmin.koch@abengoa.com

[2]IK4–IKERLAN
Technology Research Centre
Arrasate–Mondragón, Spain

[3]Dept of Energy Technology
Aalborg University
Aalborg, Denmark

***Abstract*— Connecting renewable power plants to the grid must comply with certain codes and requirements. One requirement is the ramp rate constraint, which must be fulfilled in order to avoid penalties. As this service becomes compulsory with an increased grid penetration of renewable, all possible solutions must be explored especially that large battery energy storage systems are still expensive solutions. Thus, in order to make battery investment economic viable, the use of second life batteries is investigated in the present work. This paper proposes a method for determining firstly, the optimal rating of a second life battery energy storage system (SLBESS) and secondly, to obtain the power exchange and battery state of charge profiles during the operation. These will constitute the cycling patterns for testing batteries and studying the ageing effect of this specific application. Real data from the Spanish electricity market for a whole year are used for validating the results.**

Keywords*— *Batteries, Energy storage, Optimization.

I. INTRODUCTION

Integrating large renewable energy sources (RES) power plants into the grid presents both economic and environmental benefits [1], [2]. Meanwhile, they also raise technical challenges for the grid stability and integrity due to their highly variable and intermittent characteristic.

A solution to mitigate the effects of RES high variability and enhance the stability of grids with high penetration levels of renewable power plants, is to use battery energy storage systems (BESS) connected to the grid at the same point as the RES. The BESS have a response time in the range of milliseconds [3] [4] and are able to compensate in real time the high variability of the renewable resource [5]-[7]. These systems are able to smooth the power output of the plant by reacting to the high variations in power generation and to deal with these variations by operating in charging/discharging mode in order to keep the output power ramp rate of the plant inside admissible values [3].

Before being allowed to connect and inject power to the grid, all power plants need to pass compliance tests [4]. These tests impose constraints related to the operation of the plant and their response to different grid events. Moreover, compliance tests are compulsory for the connection of the plants: passing the tests add no economic benefit, however the violation of the stated limits will bring penalties. For complying with these tests, the solution requiring the smaller initial investment is the most suited for this application. This can be achieved by minimizing the size of the battery and by reducing the cost of this storage system [8]-[11].

This paper focuses on obtaining cycling patterns for testing real Lithium-ion (Li-Ion) batteries according to the profiles obtained during simulations for a power smoothing application. The work presented in this paper is part of a European project [12] that proposes the use of second life (SL) Li-Ion batteries (retired from their first life automotive service) for a BESS (SLBESS) which provides the RES smoothing application. The driver for using SL batteries is the possibility of reducing costs and minimizing the environmental impact by using aged batteries closer to their lower operation performance. In order to obtain realistic results, the present work considers the initial state of health – for the second life application, usually around 80% of the initial BESS capacity [13], the capacity decay, and other performance characteristics of the second life batteries.

The rest of the paper is structured as follows: section II presents the requirements of the power variability smoothing service for connecting to the grid, section III presents a proposed algorithm for controlling the SLBESS in order to provide the service. Section IV presents the methodology for rating the SLBESS according to the considered application. Section V presents simulation results and discussions and section VI presents the conclusions derived from the work.

II. SLBESS POWER VARIABILITY SMOOTHING

The block diagram of the system under study for power variability smoothing is presented in Fig. 1. The plant controller is responsible of measuring the current value of the PV output power (P_{PV}) and control the SLBESS power exchange (P_{bat}) in order to maintain the plant's output power (P_{plant}) between admissible limits, according to equation 1.

$$P_{Plant}(t) = P_{PV}(t) + P_{bat}(t) \quad (1)$$

Different system operators have different requirements for connecting RES power plants to the grid. The current work focuses on the RES variability smoothing and ramp rate limits

imposed for the power plants grid connection. A ramp rate limit considered for many studies is the one defined by the

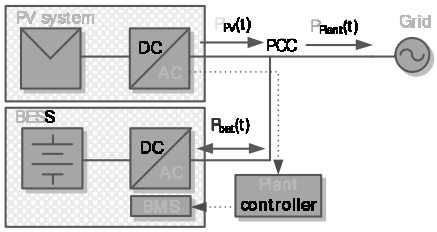

Fig. 1. Block diagram of PV variability output power smoothing application with BESS.

PREPA codes [14] as a maximum value of 10%/minute for the ramp rates [3]. In addition, in [7], the "Asociación de producatores de energia removable" (APER) has defined compliance tests for integrating RES power plants into the grid and to facilitate the interaction between the PREPA and the companies developing and operating the plants.

Of special interest for this work is the ramp rate compliance (RRC) as it is defined by the APER: the facility will be considered to be non-compliant and a curtailment penalty will be applied to the plant if the RRC is less than 98.5% during each full week. The penalty will consist of a reduction for the contracted capacity of the plant for the next week [14].

For a given time interval, the total number of compliant scans may be expressed as a percentage of all scans – this is known as RRC [7]:

$$RRC = 100\% - \frac{(\#of\ scans\ in\ violation\ of\ RR)}{(\#of\ scans\ while\ facility\ is\ generating)} \quad (2)$$

This criterion is used at the end of the paper to validate the results obtained based on the proposed rating methodology and power smoothing algorithm.

III. Battery Energy Management Algorithm

The first part in the process of assessing the required rating of the SLBESS, is to determine the control algorithm that controls the battery for providing the variability smoothing service.

In the present work, based on the least squares estimator (LSE) described in [4], a mixed least square estimator ramp rate compliant (MLSERRC) algorithm is developed. The idea of this algorithm is to include the LSE based on a parabolic estimation instead of a linear estimation complemented with the ramp rate compliance.

The MLSERRC algorithm is used as it presents better results than using the least square estimator based on linear estimation (LSE) and also than the moving average (MA) filter algorithm. Compared to MA and LSE algorithms, the use of the MLSERRC algorithm (presented in Fig. 2a) reduces the size of the BESS required to provide the output power smoothing service in addition to the ramp rate compliance service. The compared operation results between the use of a MA, LSE and MLSERRC algorithms are presented in Fig. 2 for two types of days: sunny (b, d and f) and for a day with highly variable irradiance (c, e and g).

Fig. 2b presents the PV output power (P_{PV}), the plant's smoothed output power when using the MA filter (P_{MA}), when using the LSE filter (P_{LSE}) and when using the MLSERRC algorithm ($P_{MLSERRC}$) under the same weather conditions. For providing these plant output power characteristics, the requirements in terms of power and energy for the storage system are shown in Fig. 2 d) and f), respectively. As it is presented in Fig. 2, both power and energy requirements obtained for the MLSERRC algorithm are lower than the ones obtained for the LSE and MA filters.

Similar conclusions can be drawn by analyzing the cloudy or high irradiance variable day figures, (Fig. 2c, e and g) and the MLSERRC algorithm is again the most performant, especially in case of SLBESS energy requirement.

As summary, for both types of days, the use of the MLSERRC algorithm shows better results than LSE filter and MA filter, respectively. This translates into smaller battery capacity needed and smaller power converter size needed for providing the power smoothing service which assures in the same time ramp rate compliance.

IV. Optimal Sizing of the SLBESS

For determining the optimal rating of the SLBESS, measurements taken from a real PV power plant over one year interval were used. These values are normalized according to the maximum output power recorded in the measurement vector.

For each particular day, the optimal rating of the battery was calculated as well as the power exchange profile. Consequently, the energy exchange between the battery system at the point of common coupling and the rest of the system is also calculated. For obtaining the global optimal size of the SLBESS considering the optimal values calculated for each day, a second linear optimization problem was defined and solved in order to respect the constraints imposed by the individual solutions for each day over the year.

The problem of optimally sizing the storage system is closely connected to the operation algorithm of the SLBESS. For determining the rating of the SLBESS, this paper considers the optimization program that was defined in this section. In the formulation of the optimization program, the operation of the battery storage is also optimal - assumes perfectly known conditions, as the operation of a model predictive control with perfect predictions. After the rating of the battery, the proposed MLSERRC algorithm will be used to validate the results.

The optimization program imposes constraints on the plant's output power, the battery maximum power output and the capacity of the battery. In addition, constraints regarding the capacity fade of the second life battery were introduced as well as operation limits of the battery: the maximum and minimum state of charge and state of health for the SLBESS. These constraints are defined in relations (3) - (12).

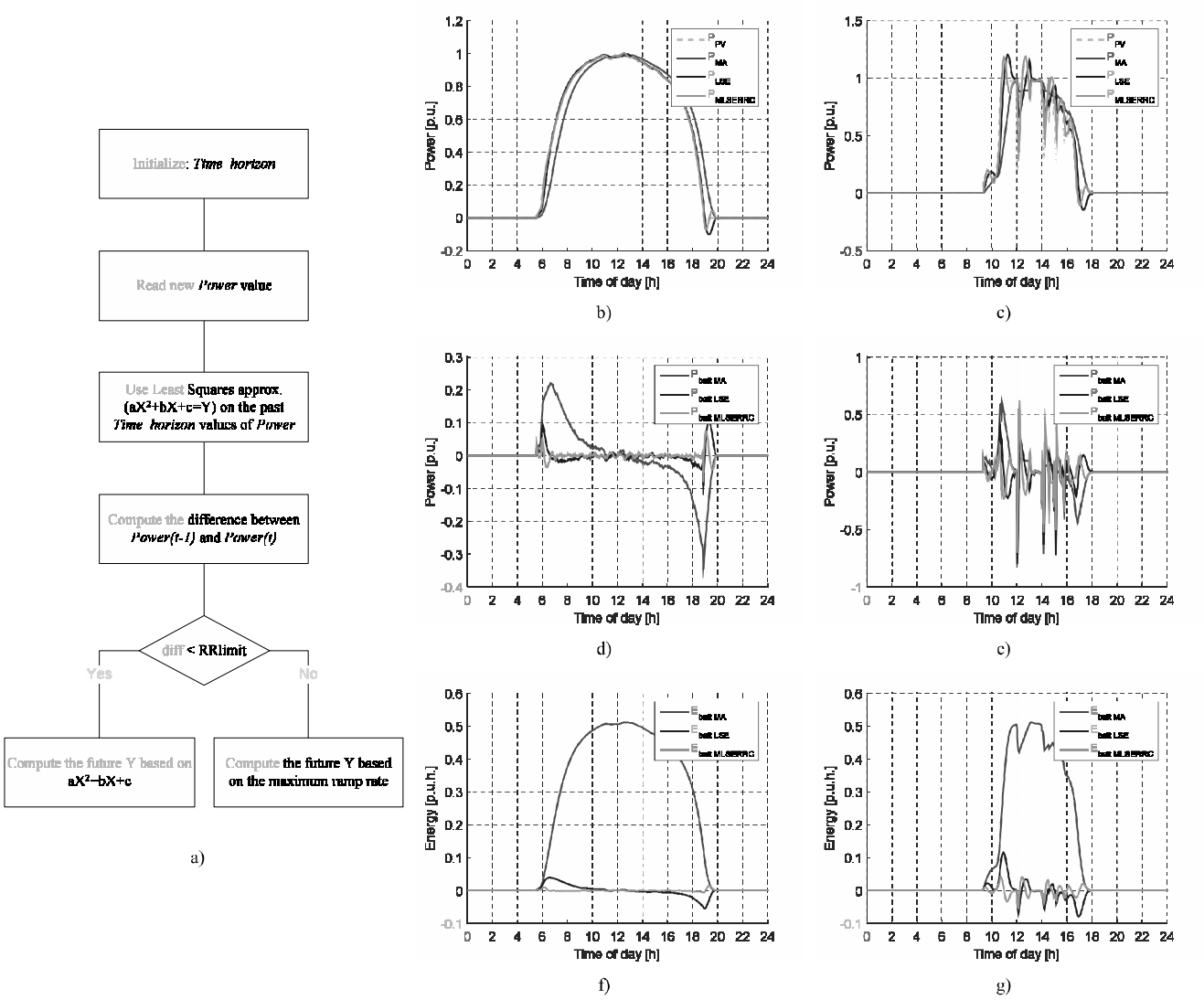

Fig. 2. The SLBESS smoothing operation algorithm: a) algorithm's diagram, PV plant output power for (b) sunny day, (c) high irradiance variable day, battery power profile (d) sunny day, (e) high irradiance variable day, battery energy profile f) sunny day and g) high irradiance variable day.

For the daily optimization problem, the following design variables were used, as specified in Table I.

TABLE I. DESIGN VARIABLES

Design Variable	Description
C_{bat}	Battery nominal capacity
$C_{ref}(t)$	Battery instantaneous reference capacity
$P_{bat}(t)$	Battery instantaneous power
$E_{bat}(t)$	Battery instantaneous energy

The use of these design variables will provide the minimum battery nominal capacity for the beginning of the second life application. That is the necessary capacity of the SLBESS to be used in the output power smoothing application. In addition, three series (vectors) of data are also generated: these are the battery instantaneous reference capacity – which due to degradation will decay in time to lower values, the battery instantaneous power and energy.

The last two design variables, P_{bat} and E_{bat}, as part of the optimization result, are describing the operation of the battery for the current simulation scenario. This result reflects the optimal operation mode of the battery, considering all the input signals (the solar irradiance values) a priori known. Based on this power exchange (P_{bat}) and rating (C_{bat}), the energy level of the battery (E_{bat}) is also provided, for each moment of the simulation interval.

The objective of the optimization program is to minimize the required capacity of the SLBESS as presented in (3) for the PV power plant ramp reduction service. The optimization program is defined in the following equalities and in-equalities:

$$\min_{C_{batt}} C_{batt} \quad (3)$$

s.t. $P_{PV}(t) - P_{PV}(t-1) + P_{bat}(t) - P_{bat}(t-1) \leq \text{ramp\_rate\_limit}$ //ramp up limit constraint (4)

$-P_{PV}(t) + P_{PV}(t-1) - P_{bat}(t) + P_{bat}(t-1) \leq \text{ramp\_rate\_limit}$ //ramp down limit constraint (5)

$-\frac{1}{\text{meas}_{freq}} P_{bat}(t) + E_{bat}(t) - SOC_{max} C_{ref}(t) \leq 0$ // SoC upper constraint (6)

$\frac{1}{\text{meas}_{freq}} P_{bat}(t) - E_{bat}(t) + SOC_{min} C_{ref}(t) \leq 0$ // SoC lower constraint (7)

$SOH_{min} \cdot C_{batt} - C_{ref}(t) \leq 0$ // Cref upper constraint according to SOH of the initial battery (8)

$-SOH_{max} \cdot C_{batt} + C_{ref}(t) \leq 0$ // Cref lower constraint according to SOH of the initial battery (9)

$C_{ref}(t) - C_{ref}(t-\Delta t) \leq 0$ // the decay constraint of the Cref (10)

$C_{ref}(t) - C_{ref}(t-\Delta t) \leq -Z \cdot [E_{bat}(t-\Delta t) - E_{bat}(t)]$ // the decay rate constraint of the Cref (11)

$-P_{bat} + P_{PV}(t) \leq 0$ // constraint on battery charging (12)

$E_{bat}(t) - E_{bat}(t-\Delta t) - P_{bat}(t) \cdot \Delta t = 0$ // SLBESS energy level during operation (13)

where the following variables were used:

$P_{PV}(t)$ –the instantaneous PV output at time instant t. [p.u.]

$P_{bat}(t)$ –the battery instantaneous power at time instant t. [p.u.]

ramp_rate_limit –the ramp rate constrain to be considered at the output of the power plant. For this study case, this limitation is set to be 10%/min. [p.u.]

meas_{freq} –the sampling frequency; for this case a measurement is taken each 2 minutes.

SOC_{min} –the minimum value for the state of charge. For second life battery this value is considered 20 [%] in relation to battery initial capacity C_{bat}.

SOC_{max} –the maximum value for the state of charge. For second life battery this value is considered 80 [%] in relation to battery initial capacity C_{bat}.

SOC_{ini} –the initial SOC of the battery [%]. This value is introduced as initialization.

C_{batt} – the battery's initial capacity. [p.u.h.]

C_{ref} – the capacity reference for each sampling time. This will decay in time. [p.u.h]

SOH_{min} – the minimal value of state of health of the battery resulting from the first life application [%]. For this second life application, the 80% value is considered.

SOH_{max} –the maximal value of state of health of the battery. [%]

Z – the capacity fade coefficient correlated to the battery discharge process.

The correct assignment of some of these variables entails knowing some of the most relevant battery performance characteristics. Considering that in this case, the scope of the sizing process is to obtain representative power profiles and cycling patterns for a later battery testing, it is difficult to provide precise values for some of these variables.

In this way, the maximum and minimum SOH limits (SOH_{max}, SOH_{min} respectively) have been assigned according to typical values reported in literature for second life batteries [16]. The widespread SOH value at which the batteries are typically expected to be retired from the automotive use is 80%, which in this case has been used as SOH_{max}=80% [16]. Similarly, the SOH value at which the batteries would be retired from the second life use has been established as SOH_{min}=64% of the nominal battery capacity, when installed in the EV, or 80% of the battery capacity initially available in the second life SOH_{max} (which has been assumed to be 80% of the nominal capacity as already mentioned). This is above the 50% retirement criteria established by Neubauer and Pesaran in [17].

Similarly, determining the BESS maximum and minimum power capabilities implies assuming certain hypothesis that will not be validated until the batteries are subjected to real testing. However, considering batteries' pulse power capabilities, measured by means of pulse power characterization testing at the beginning of life (BOL) of the cells considered in this analysis, it was decided to establish an operating range from SOC_{min}=20% to SOC_{max}=80%. The cells used for this analysis are 20Ah high-energy NMC-based commercial cells. These cells will be later subjected to second life testing with the power profiles obtained from the results of the sizing study presented in this paper.

As shown in Fig. 3, the power capabilities of such cells, calculated according to equation (14) are considerably lowered

below 20% SOC [18]. In absolute values, this will be even more evident as cell degrades. This work models the SOC referring to the current capacity of the battery and not with the initial one. On the other hand, it was also considered that the useful life of the second life batteries will be enhanced by limiting the operation range to a maximum 60% cycle depth, which leads to the mentioned 20% - 80% SOC interval. Even though the operating limits established may seem conservative taking BOL characteristics into account, it is expected that cell power and energy capabilities will be considerably lowered before being used in the considered second life application.

$$P = i^2 \cdot \frac{\Delta v}{\Delta i} \tag{14}$$

Where P is the power capability of the cell, i is the current during the pulse, Δv is the voltage change during the 10s of current pulse, and Δi is the current change during the 10s current pulse.

On the other hand, determining an accurate capacity fade coefficient (Z) requires inevitable cell testing and a battery ageing model. Thus, considering the particularity of the case here explained, where this coefficient needs to be somehow established before the cells are subjected to ageing tests, it was decided to use the capacity fade coefficient calculated for the first life ageing, assuming that the ageing mechanisms governing cell performance in the first life will continue being the same along the second life; however, this assumption needs to be validated after second life battery testing.

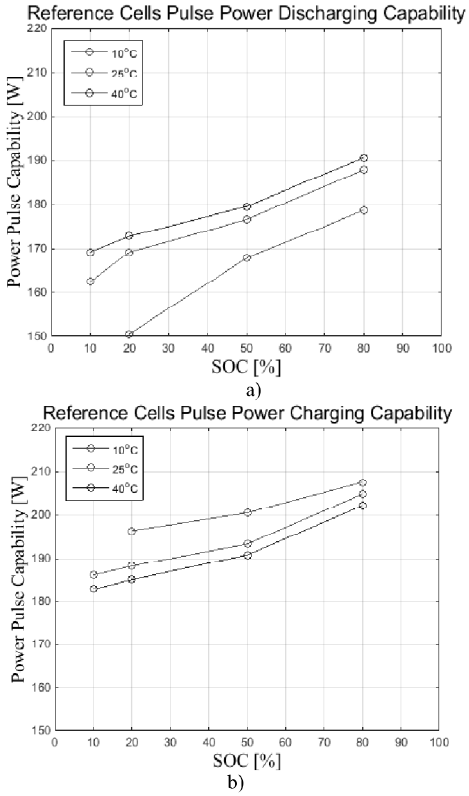

Fig. 3. Battery discharging (a) and charging (b) pulse power capabilities measured at BOL for different temperatures

As a result, the daily optimal size of the SLBESS is obtained. Depending on the conditions of each day, these values can differ significantly from cases where the use of the battery is not necessary, to days that require a 0.06 (p.u.h) of battery storage, as shown in Fig. 4a.

Initial conditions regarding the capacity, reference capacity of the battery, and the initial battery energy are modeled by the following in-equalities:

// C_{batt} and C_{ref}:

$$C_{ref}(1) - SOH_{ini} \cdot C_{bat} \leq 0 \tag{15}$$

// Initial capacity decay:

$$C_{ref}(1) - SOH_{ini} \cdot C_{bat} - Z \cdot [E_{bat}(1) - SOH_{ini} \cdot SOC_{ini} \cdot C_{bat}] \leq 0 \tag{16}$$

// Initial battery energy:

$$E_{bat}(1) - SOH_{ini} \cdot SOC_{ini} \cdot C_{bat} - P_{bat}(1) = 0 \tag{17}$$

An initial assumption that the battery SOC has the same initial value at the beginning of each day can be justified by the fact that the battery's controller can easily bring the battery to this SOC value during the day when power is available from the PV system. The battery enters an "initial SOC" mode of operation and charges from the PV or discharges into the grid the energy difference until SOC_{ini} is reached. The described optimization program is developed in MATLAB.

V. Results and Discussions

At first, an analysis of the ramp rates for the available one year measurement data presents the initial conditions of the PV power plant prior to the use of the SLBESS for the variability smoothing service. As mentioned in Section II, the ramp rate limit that the plant must provide is 10%/ minute (or, based on the available 2 minutes sample measurements, 20%/ 2minutes).

Fig. 4a presents the ramp rate of the PV output before using the SLBESS as well as the results when using the smoothing application as a result of the global optimization. Fig. 4b presents a statistical insight regarding the frequency distribution of different ramp rates over the one year available data.

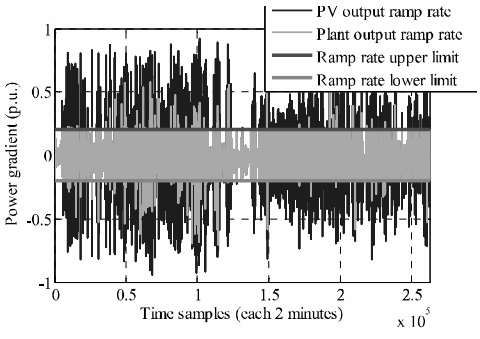

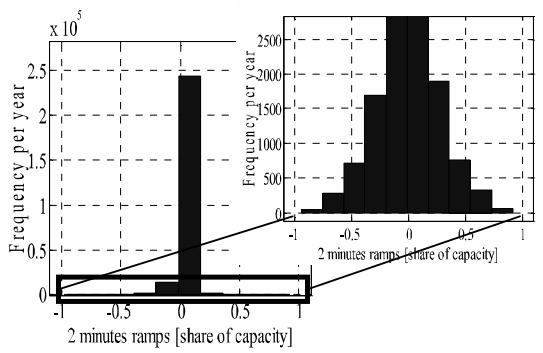

b)

Fig. 4. Yearly output power ramp rate analysis: a) the output power ramp rate of the PV system and of the plant when the MLSERRC algorithm is used and b) the distribution diagram of power ramp rates of different magnitudes over the entire year.

Using the optimization program defined in Section III, the daily optimal values for the variability smoothing application were obtained. These values are plotted in Fig. 5. It can be seen that there are different values required for the battery capacity depending on the day of the year to provide the smoothing service during one year of operation. For achieving the ramp rate constraints defined in Section II; the nominal capacity of the SLBESS is obtained based on the daily optimal values and battery energy charge/discharge profiles. This process is illustrated in Fig. 5. The initial optimal value of the C_{ref} was obtained as the minimum value that provides the necessary capacity for the battery to achieve the power smoothing throughout the entire year, considering the capacity fade characteristics and the daily optimal value constraints. This figure presents the decay of the battery starting from the initial value during one year of operation.

The solution of the optimization problem, representing the optimal operation case, was used to simulate the operation using the MLSERRC algorithm presented in Section III for assessing the real operation and validity of the obtained result.

For testing the performance of the proposed algorithm and to validate the results obtained by utilizing the optimization program, the RRC assessment proposed by APER in [7] was used. As stated in Section II, a curtailment penalty will be applied to the plant if the RRC is less than 98.5% during a week.

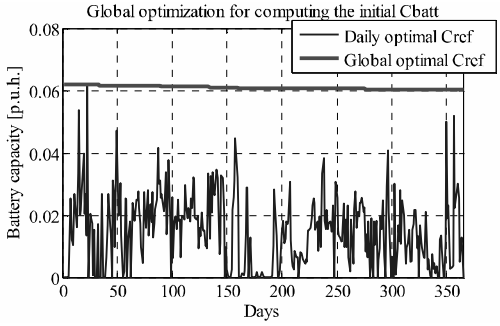

Fig. 5. Daily optimal values for Cref and the rating of the battery according to capacity decay.

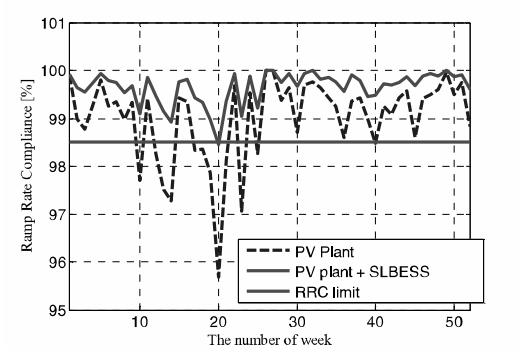

Fig. 6. The Ramp Rate Compliance (RRC) for the PV plant when the plant is directly connected to the grid and when the SLBESS is used for the output power smoothing.

Fig. 6 represents the RRC computed for the plant as stated in (2). The RRC is computed for each week of the one year interval for two cases: the initial PV plant generating power according to the variable nature of the solar irradiance and the second case corresponding to the plant operating with the SLBESS. The SLBESS is rated by utilizing the optimization program. Although the optimization is implemented considering perfectly known energy production conditions (the optimal case), for evaluating the performance of the SLBESS calculated on a realistic working scenario, the algorithm used was the MLSERRC, as described in Section III.

From the Fig. 6 it is seen that the RRC limits are not violated and the plant operates without penalties.

As the optimization program considers the optimal operation (a perfect predicted scenario) the resulting capacity of the battery (0.0612 p.u.h.) must be checked according to the defined MLSERRC operation algorithm, for testing its evolution when battery system is ageing (Fig. 7) and assess the RRC as defined in (2).

Fig. 7 presents the operation of the SLBESS during one year, by using the initial capacity obtained from the optimization program when using the MLSERRC algorithm for the operation of SLBESS. The battery stored energy level is kept between the limits imposed by the battery energy management, defined as SOC_{min} (20%) and SOC_{max} (80%). Another aspect noticeable in this operation scenario is the battery's capacity decay over time, as a result of the battery operation.

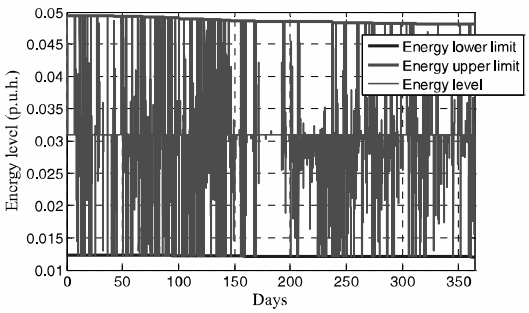

Fig. 7. The SLBESS energy status during one year when using the MLSERRC algorithm for variability smoothing.

The SL batteries used for this application have an initial state of health (SOH) of around 80%, the state at which the first life application – e.g. the automotive application – considers these batteries to be at the end of life.

VI. Conclusions

The current work presents a generic method for the integration of RES power plants by using SLBESS for providing variability smoothing service for a PV power plant. The choice of second life batteries for this service represents a cost effective alternative solution for the use of new storage systems. However, the applied optimization strategy is applicable also for a new battery system (first life).

By using the proposed optimization method consisting in real measurements taken from a PV plant for the duration of a year, the optimal rating for a SLBESS is achieved. In addition, the study uses a new variability smoothing algorithm for emulating the operation conditions of the SLBESS during the entire year operation.

Furthermore, the analysis performed allows obtaining power profiles and cycling patterns representative of the application considered, building a basis for experimental testing of second life batteries.

The power profiles obtained from this study will later be used for second life battery testing, which will allow analyzing the performance capabilities of such batteries, and their ageing behavior when used for providing power variability smoothing.

Acknowledgment

This work is funded by the European Union through the NMP.2013-1 Batteries2020 project (Grant agreement GC.NMP.2013-1 /GA nº 608936).

References

[1] S. Chowdhury, S. P. Chowdory, and P. Crossley. *Microgrids and active distribution networks.* IET Renewable energy series. United Kingdom. 2009.

[2] S. Vazquez, S. M. Lukic, E. Galvan, L. G. Franquelo, and J. M. Carrasco, "Energy storage systems for transport and grid applications," IEEE Trans. Ind. Electron., vol. 57, no. 12, pp. 3881–3895, Dec. 2010.

[3] ENSTSO-E, "Network Code for Requirements for Grid Connection Applicable to all Generators," Tech. Rep., 2013. [Online]. Available: www.entsoe.eu.

[4] C. Gavriluta, I. Candela. J. Rocabert, Etxeberria-Otadui, P. Rodriguez, "Storage system requirements for grid supporting PV-power plants," Energy Conversion Congress and Exposition (ECCE), 2014 IEEE , vol., no., pp.5323,5330, 14-18 Sept. 2014.

[5] J. Marcos, O. Storkël, L. Marroyo, M. Garcia, E. Lorenzo, "Storage requirements for PV power ramp-rate control", Solar Energy, Volume 99, Pages 28-35, January 2014.

[6] W. Guishi. M. Ciobotaru, V.G. Agelidis, "Power Smoothing of Large Solar PV Plant Using Hybrid Energy Storage," Sustainable Energy, IEEE Transactions on , vol.5, no.3, pp.834,842, July 2014.

[7] APER, "Minimum technical requirements compliance procedure proposal", Tech. Rep., 2014 [Online]: http://www.aperpr.com/wp-content/uploads/2014/08/MINIMUM_TECHNICAL_REQUIREMENTS_COMPLIANCE_PROCEDURE_PROPOSAL_JUL2013.pdf

[8] A. Etxeberria, I. Vechiu, H. Camblong, and J. M. Vinassa, "Hybrid energy storage systems for renewable energy sources integration in microgrids: A review," in Proc. IPEC, pp. 532–537, 2010.

[9] A. Arabali, M. Ghofrani, M. Etezadi-Amoli, M.S. Fadali, "Stochastic Performance Assessment and Sizing for a Hybrid Power System of Solar/Wind/Energy Storage," Sustainable Energy, IEEE Transactions on , vol.5, no.2, pp.363,371, April 2014.

[10] L. Xiangjun, H. Dong, L. Xiaokang, "Battery Energy Storage Station (BESS)-Based Smoothing Control of Photovoltaic (PV) and Wind Power Generation Fluctuations," Sustainable Energy, IEEE Transactions on , vol.4, no.2, pp.464,473, April 2013.

[11] H. Beltran, M. Swierczynski, A. Luna, G. Vazquez, E. Belenguer, "Photovoltaic plants generation improvement using Li-ion batteries as energy buffer," Industrial Electronics (ISIE), 2011 IEEE International Symposium on , vol., no., pp.2063,2069, 27-30 June 2011.

[12] Batteries2020 project webpage: http://www.batteries2020.eu/.

[13] USABC. Electric vehicle battery test procedures manual-revision 2, 1996. Available online: http://avt.inl.gov/battery/pdf/usabc_manual_rev2.pdf

[14] PREPA, 2012. Puerto Rico Electric Power Authority Minimum Technical Requirements for Photovoltaic Generation (PV) Projects. <http://www.fpsadvisorygroup.com/rso_request_for_quals/PREPA_Appendix_E_PV_Minimum_TechnicalRequirements.pdf.> (accessed November 2014).

[15] Y. Yongheng, W. Huai; F. Blaabjerg, T. Kerekes, "A Hybrid Power Control Concept for PV Inverters With Reduced Thermal Loading," Power Electronics, IEEE Transactions on , vol.29, no.12, pp.6271,6275, Dec. 2014.

[16] S. Saxena, C. Le Floch, J. MacDonald, S. Moura, "Quantifying EV battery end-of-life through analysis of travel needs with vehicle powertrain models", Journal of Power Sources, Volume 282, 15 May 2015, Pages 265-276.

[17] J. Neubauer, A. Pesaran, "The ability of battery second use strategies to impact plug-in electric vehicle prices and serve utility energy storage applications", Journal of Power Sources, Volume 196, Issue 23, 1 December 2011, Pages 10351-10358.

[18] ISO 12405-2:2012, "Electrically propelled road vehicles – Test specification for lithium-ion traction battery packs and systems – Part 2: High-energy applications", July 2012.